

Is motion processing unitary?

William A. Simpson and Velitchko Manahilov

Vision Sciences Department, Glasgow Caledonian University, Cowcaddens Road, Glasgow G4 0BA, Scotland

Melissa S. Mair

Psychology Department, University of Winnipeg, 515 Portage Avenue, Winnipeg MB, Canada R3B 2E9

Received March 9, 1999; accepted June 22, 1999; revised manuscript received July 21, 1999

Motion discrimination space is conventionally categorized into motion detection, speed discrimination, and direction discrimination tasks. But an ideal observer uses a unitary motion mechanism that is affected only by the noise level and the difference in speed (or displacement) between two stimuli. We tested whether human performance in the various motion tasks showed the working of a unitary mechanism or the combined outputs of more than one mechanism. We examined the whole motion discrimination space, using random dots that underwent a sudden jump or displacement. The discriminability was measured as a function of the standard and comparison displacements. Both the ideal observer model and a nonideal observer model that contains additive internal noise predict a planar response surface. When the dot motion was noiseless, the planar surface fitted well except for much higher than expected sensitivity for motion detection. This is consistent with a purely temporal mechanism that uses flicker or a purely spatial mechanism that uses the length of time-averaged streaks. It is also consistent with a Weber's law device. When motion noise was added to the displays, the planar response surface again fitted well, although the residuals showed the presence of a speed energy mechanism. We conclude that a unitary motion mechanism exists (nonideal observer model), although its performance may be supplemented by other mechanisms whose main impact is on discrimination of speeds near zero. © 1999 Optical Society of America [S0740-3232(99)00212-4]

OCIS codes: 330.4150, 330.5510, 330.4060.

1. INTRODUCTION

Human motion sensitivity can be measured by several different sorts of experiment. In a motion detection experiment¹ the observer discriminates moving and stationary displays. In a speed discrimination experiment, the observer discriminates a larger and a smaller speed, both in the same direction.² Finally, in a direction discrimination task, the two speeds have the same magnitude but opposite directions.³ Do all these tasks tap one and the same mechanism?

To an ideal motion observer all the tasks are alike. The ideal observer's performance depends only on the amount of noise and the size of the speed or displacement difference. In our experiments we use a sudden jump or displacement. A random dot field that jumps rightward by 2 arcmin can be described as delivering either a positional step of 2 arcmin or a speed of 2 arcmin s⁻¹ (since an impulse is in units of s⁻¹). To an ideal observer a rightward jump of 2 arcmin and a leftward jump of 2 arcmin (direction discrimination) would be as discriminable as a rightward jump of 4 arcmin and a stationary display (motion detection), which in turn would be as discriminable as a rightward jump of 2 arcmin and a rightward jump of 6 arcmin (speed discrimination); in all cases the displacement difference is 4 arcmin. We shall develop the ideal observer model in detail shortly.

The ideal observer model uses a unitary motion-sensing mechanism. However, in a real observer, the various motion tasks may tap several distinct mechanisms. The whole response surface could be a patchwork, with each patch being contributed by a different

mechanism. Motion detection stimuli, which contain nonmotion cues, could tap a position-based mechanism.⁴ Direction discrimination stimuli may tap an opponent-motion mechanism, and this mechanism may not work for speed discrimination stimuli that move in the same direction. Thus the shape of the response surface may depend on factors other than just the speed (or displacement) difference.

We compared the performance of observers in the different motion tasks. The experimental layout is shown in Fig. 1. Each cell of the figure corresponds to one experimental condition. In each condition, the standard and the comparison jumps were presented, and the observer's ability to discriminate them was measured with the signal-detection-theory index d' . The various motion tasks fall in patches of the experimental matrix. When the standard or comparison jump is zero, we have a motion detection task. When the jumps have equal magnitudes but are in opposite directions, we have a direction discrimination task. When both jumps are in the same direction but have different magnitudes, we have an ordinary speed discrimination task. When the jumps differ in both direction and magnitude, we call it a "combo" task because it combines aspects of the direction discrimination and speed discrimination tasks.

By adding motion noise to the displays, we were also able to measure the efficiency of the observer in discriminating the stimuli in the various tasks. If motion processing is unitary, we might expect the efficiency to be the same regardless of the task. Conversely, if multiple mechanisms process the motion, we expect a pattern of ef-

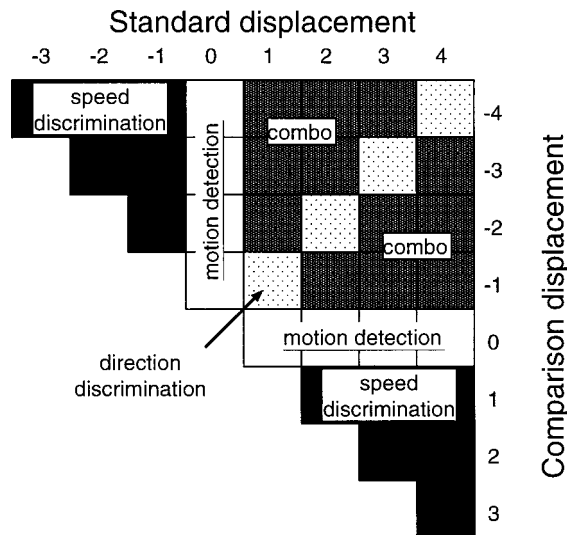


Fig. 1. Each cell in the diagram shows an experimental condition: a pair of standard and comparison displacements to be discriminated, in arbitrary units. Detectability d' for discriminating each pair was measured.

iciencies that reveals these mechanisms. The efficiency was found by comparing the performance of the real observers to that of an ideal observer. Let us now derive the performance of an ideal observer.

2. IDEAL-OBSERVER ANALYSIS

The situation that we analyze is known as a “multiple sample binary communication system.”⁵ There are two speed signals to be discriminated: the vectors \mathbf{s}_0 and \mathbf{s}_1 (each consisting of m time samples). At each instant a sample of normal $N(0, \sigma^2)$ noise, n_k , is added to the signal. The ideal observer knows the two signal waveforms exactly and performs the discrimination by cross correlating the received (signal + noise) waveform with each of the two signals. The discriminability of the standard and comparison speeds is given by

$$d' = \frac{\left[\sum_{k=1}^m (s_{1k} - s_{0k}) \right]^{1/2}}{\sigma}. \quad (1)$$

This equation holds for any pair of signals. In our experiments the speed signals were

$$s_{0k} = a_0 \delta_{k-T} = \begin{cases} a_0 & \text{if } k = T \\ 0 & \text{if } k \neq T \end{cases} \quad (2)$$

$$s_{1k} = a_1 \delta_{k-T} = \begin{cases} a_1 & \text{if } k = T \\ 0 & \text{if } k \neq T \end{cases} \quad (3)$$

Each signal is a Kronecker delta function⁶: The speed is zero except for an impulsive jump having a speed (or displacement) a_0 or a_1 at time T . The discriminability of these signals is

$$d' = \frac{[(a_1 - a_0)^2]^{1/2}}{\sigma} = \frac{|a_1 - a_0|}{\sigma}. \quad (4)$$

For each pair of comparison and standard speeds (displacements) we measured the discriminability. According to the ideal observer analysis, the d' points should lie on the surface of a tilted plane that passes through the origin. (The surface is actually V shaped, but in our experiments we looked at just one of its two symmetrical planes.)

An ideal observer would discriminate noiseless displays perfectly, with infinite d' . We can model the results for noiseless displays if we suppose that the observer's visual system contains motion noise. The noise would likely be due to variability in the observer's fixation as well as in the output of neurons coding the displacement. The nonideal-observer model prediction is also Eq. (4), but now we interpret σ as representing the standard deviation of the internal noise. In the case of a noisy display, σ is the square root of the sum of internal and external noise variances. This nonideal observer model predicts that the detectability surface will be a tilted plane passing through the origin.

In our experiments we presented only horizontal motion. In general, motion has a vertical component as well. If both components were present, the ideal and the nonideal observer models would discriminate the displacement or velocity vectors \mathbf{a}_0 and \mathbf{a}_1 .

3. METHOD

A. Observers

The authors, WS, VM, and MM, served as observers. VM has normal vision; MM and WS have corrected-to-normal vision.

B. Apparatus

The displays were presented on a Tektronix 608 oscilloscope with P15 phosphor. The oscilloscope was controlled by a point-plotting memory buffer developed at the University of Alberta.⁷ Viewing was binocular from a chin rest placed 86 cm from the face of the oscilloscope. A button box collected responses.

C. Stimuli

The stimulus consisted of bright (202 cd/m^2) moving random dots on a black (0.001 cd/m^2) background. There were 990 random dots and a fixation cross at the center made up of 10 dots; thus there were 1000 dots in total. Since the dots were plotted at a rate of one per microsecond, the refresh rate of a frame was 1000 Hz. The random dots filled a 4.1-deg-square region. Each dot was 2.8 arcmin in diameter.

Two versions of the experiment were run. In the noiseless experiment, the display was a two-frame horizontal motion sequence with wraparound. Each frame was displayed for 200 ms. Several displacements were used in the range ± 1.92 arcmin. Given the properties of the Dirac delta function, the speed was in the range $\pm 1.92 \text{ arcmin s}^{-1}$. The average speed over the duration of the display was $\pm 4.80 \text{ arcmin s}^{-1}$.

The noisy experiment was similar, with a single horizontal jump as the signal (displacements in the range ± 3.84 arcmin), but horizontal-motion noise was superimposed on the display. The display used 80 frames, each

displayed for 5 ms. It is easiest to describe the display by separating the signal and noise components. The signal was a single horizontal jump, generated by moving each dot i from position x_i on frames 1–40 (200 ms), to position $x_i + \Delta$ on frames 41–80 (200 ms). A new sample of normal random noise with mean zero and standard deviation 0.3 arcmin was added onto each dot's horizontal position on each frame. The noise added on each frame was the same for all the dots. This gave the display a rigid jittering similar to fixation noise.⁸ Since the average speed of the noise was zero, the average speed of the display was the same as in the noiseless case (in the range ± 4.80 arcmin s^{-1}).

D. Procedure

In a block of trials the observer was presented with two stimuli: the standard and the comparison jumps. Each trial contained either the standard or the comparison, and the observer indicated by a button press which had occurred. The standard and the comparison were presented in random order. A block with a given standard and comparison consisted of 100 trials. Five blocks of trials were run for each stimulus pair for the noiseless condition, and four blocks were run for the noisy condition.

At the beginning of a block of trials, the observer was familiarized with the standard and comparison stimuli by seeing them presented in alternation three times each. When ready, the observer then initiated the experiment proper. Each response was categorized as a hit (response of "standard" when standard was presented), miss (response of "comparison" when standard was presented), false alarm (response of "standard" when comparison was presented), or correct rejection (response of "comparison" when standard was presented). Auditory feedback followed each incorrect response.

4. RESULTS AND DISCUSSION

We presented pairs of standard and comparison jumps and measured their discriminability d' . These discriminations were performed for displays with and without superimposed motion noise. The data form a surface whose shape we can compare to an ideal motion observer that uses a unitary mechanism. The data from the noisy displays allow us to evaluate the efficiency of motion processing, which sheds light on the unitary motion processing issue as well as being of intrinsic interest.

A. Unitary Motion Sensing?

If motion sensing uses a unitary mechanism, the ideal and the nonideal observer models predict a detectability surface that is a tilted plane passing through the origin. The models are unitary in that the discriminability of a pair of jumps should depend only on the difference in the sizes of their displacements and the noise level. Our approach is to fit the ideal and the nonideal observer models to the data and then to look at the errors (residuals). If motion sensing is unitary and is well described by the ideal or the nonideal observer model, then the error surface will be flat with random deviations. On the other hand, if each task—motion detection, speed discrimination, direction discrimination, combo—taps a different

mechanism, we will expect a surface with bumps or dips that deviate from the plane. The errors will not be random; the error plot will have a systematic nonflat surface. A systematic error surface indicates the presence of extra mechanisms operating in addition to the ideal or the nonideal observer mechanism. The logic is simple. We have data = fit + error, where the fit is due to the ideal or the nonideal observer model. In the case in which the ideal or the nonideal observer model fits well, the error is due to sampling or measurement. We explain the data by one mechanism, the ideal or the nonideal observer model. In the case where there are systematic bumps or dips in the error surface, the error term does not represent sampling error but instead represents the contribution of another mechanism (or mechanisms). Each observed d' is the sum of the d' output by the ideal observer mechanism and the d' output by an additional mechanism.

1. Noiseless Displays

Figure 2 shows the measured d' surfaces for the noiseless displays. The ideal observer model cannot be fitted if there is no noise in the display, so we fitted the nonideal observer model [Eq. (4)] by using least squares. The nonideal observer model predicts that the detectability surface will be a tilted plane passing through the origin.

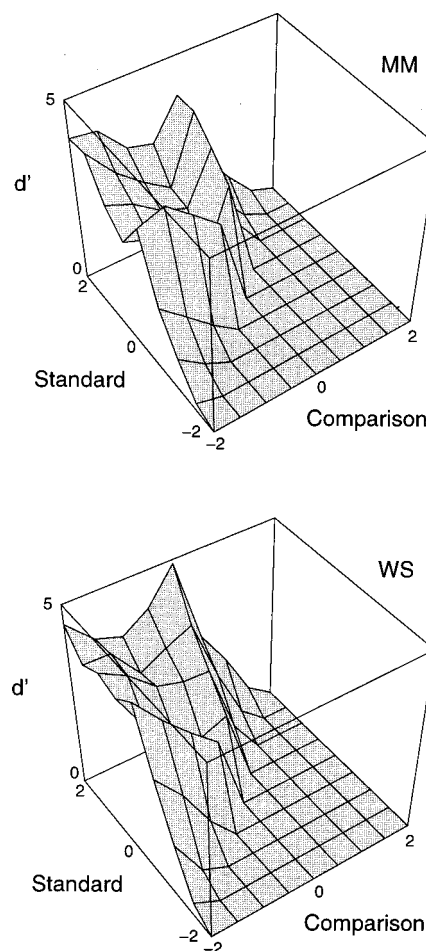


Fig. 2. Detectability d' of the difference between the standard and comparison displacements (arcmin) for observers MM and WS. The display is noiseless.

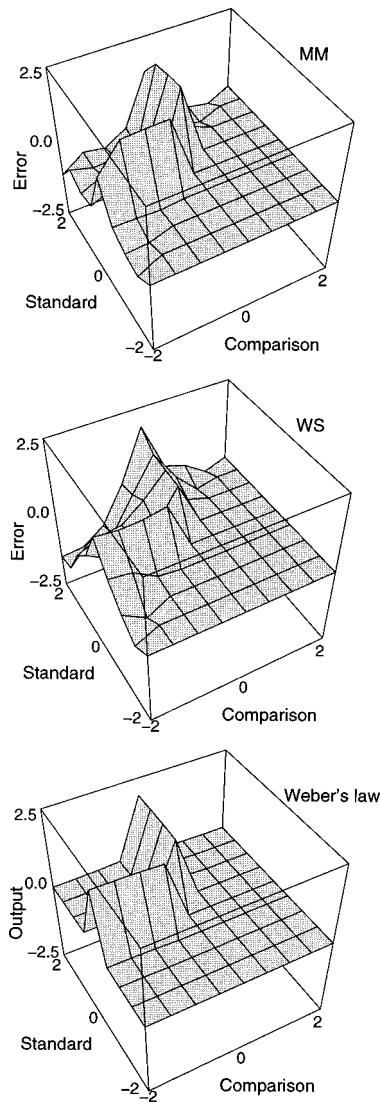


Fig. 3. Error—difference between observed and best-fitting values of d' with use of Eq. (4)—as a function of the standard and comparison displacements (arcmin) for observers MM and WS and a device that obeys Weber's law. The display is noiseless. In this and subsequent figures the region where the surface was not measured is given a height of zero to serve as a visual reference.

The obtained surface has more or less the appearance of a tilted plane, but for both observers the plane has a superimposed ridge, which will discuss shortly. The nonideal observer model has only one parameter, the standard deviation of the noise inside the observer's visual system. For observer MM the 95% confidence interval for the internal noise standard deviation is 0.76 ± 0.07 arc min, and for observer WS the estimate is 0.65 ± 0.05 arc min.

The nonideal observer model does not completely describe the data. There is an L-shaped ridge that is made very clear by the residual plot in Fig. 3. The residual plot shows the difference between the obtained d' s and those predicted by the best-fitting nonideal observer model. The ridge corresponds to the motion-detection task: If the standard or the comparison is zero (stationary), performance is much higher than predicted by the model.

We conclude two things from Figs. 2 and 3. First, the nonideal observer model is good as a first approximation. It is able to describe the results from the direction discrimination, speed discrimination, and combo tasks quite well—the residual plot is flat for these conditions. However, and this is the second conclusion, the performance of the real observer is much better for the motion detection task than we would predict from the nonideal observer model. The response surface is the sum of the plane due to the nonideal observer mechanism and the ridge due to another mechanism. The nonideal observer mechanism is always at work, but an extra mechanism is recruited when one of the sequences being discriminated is stationary.

Our analysis so far has been at a high level of abstraction. We have stated that a nonideal observer mechanism and a mechanism specialized for static displays exist, but we have given no details about how these mechanisms extract information from the stimuli. Let us first consider how the nonideal observer mechanism might extract the needed information. A traditional idea⁹ is that the position of an object is found at successive instants, and the difference is taken to find the displacement. This idea does not spell out how the position of the object is computed; this information has to be extracted from the time-varying luminance distribution $L(x, y, t)$ delivered to the retina. Other sorts of mechanisms that extract the motion from $L(x, y, t)$ have been proposed.^{10,11} Any mechanism that extracts the speed or displacement is compatible with the nonideal observer model.

What is the basis of the mechanism specialized for static displays? One possible mechanism is based on time averaging.¹² The mechanism works like a long-exposure photograph of a moving scene (Fig. 4). If the dots are static, the output of the mechanism is a set of dots. If the dots move, the output is a set of streaks. So the observer's rule is, if streaks, say "motion"; if dots, say "static." Such a mechanism will work well for motion detection and not at all for direction discrimination. The time averager is a purely spatial mechanism. A purely temporal mechanism based on flicker could also be at work. Any given point in the static display is constant over the display period, whereas for the moving dots, individual locations flicker on and off. The mechanism will simply test for the presence of flicker to perform motion detection. This flicker mechanism's performance will not depend on the displacement. The ridge in the residual plot (Fig. 3) has a constant height regardless of the displacement, and so the flicker mechanism seems plausible. A final possibility is that the ridge is produced by a mechanism that obeys Weber's law.² In an experiment in which a_0 is varied and the value of a_1 just discriminable from a_0 is measured, Weber's law can be written as

$$|a_0 - a_1| = \sigma + |a_0|\sigma_1, \quad (5)$$

where σ is the standard deviation of the internal noise or, in other words, the motion detection threshold, and σ_1 is the Weber fraction. If instead a_1 is varied and the value of a_0 just discriminable from a_1 is measured,

$$|a_0 - a_1| = \sigma + |a_1|\sigma_1. \quad (6)$$

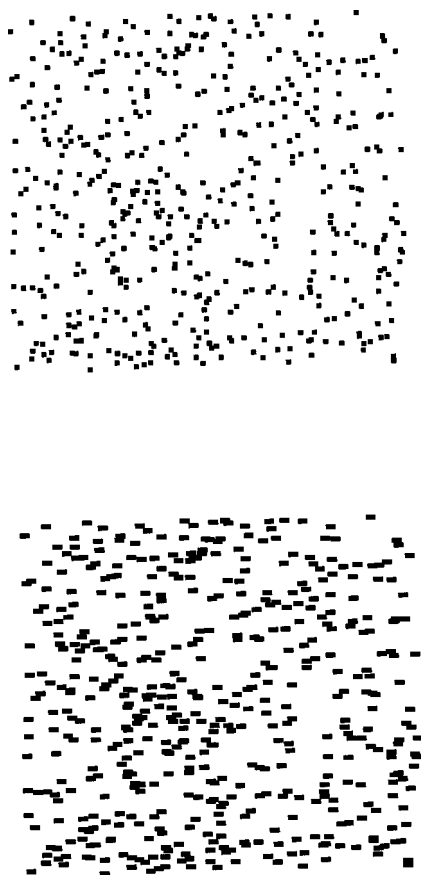


Fig. 4. Time-averaging mechanism giving an output like that of a long-exposure photograph. This mechanism can perform motion detection by comparing the output for static random dots (top) with the streaks obtained for moving random dots (bottom).

We eventually want an expression for the discriminability of the pair a_0 and a_1 , so we need to combine Eqs. (5) and (6) in some way. One way to do it (using the idea of separable functions) is

$$|a_0 - a_1| = (\sigma + |a_0|\sigma_1)(\sigma + |a_1|\sigma_1). \quad (7)$$

Since $d' = 1$ at threshold, we have

$$d' = \frac{|a_0 - a_1|}{(\sigma + |a_0|\sigma_1)(\sigma + |a_1|\sigma_1)}. \quad (8)$$

This surface is shown at the bottom of Fig. 4, and it can be seen that the Weber's law prediction matches the residuals quite well. So a simple account of the data is that they are the combined output of a nonideal (noisy) observer and a Weber's law device.

The logic of our analysis attributes deviations from the nonideal observer models to a secondary mechanism. Could our response surfaces instead be revealing a single mechanism? Could a single mechanism produce both the plane and the ridge? The answer depends on what one calls a mechanism. In our view, a mechanism is a functional unit that is defined by how it extracts information from the stimulus needed to perform some task. The task in our experiments is to discriminate two signals, and the best possible information extraction mechanism for this task is the ideal observer. The ideal observer is a natural and nonarbitrary starting point in constructing a

functional decomposition of the system. The planar part of the response surface corresponds to the ideal observer (with additive internal noise). The ridge does not correspond to the ideal observer and so is due to some other mechanism. Suppose a single motion sensor was constructed that produced the response surface that we observe. We would say that regardless of the details of the construction, such a motion sensor consists of two functional parts: one part that acts as a nonideal observer and another that exhibits Weber's law behavior.

2. Noisy Displays

The pattern of results is similar for displays that have added motion noise. As shown in Fig. 5, the detectability

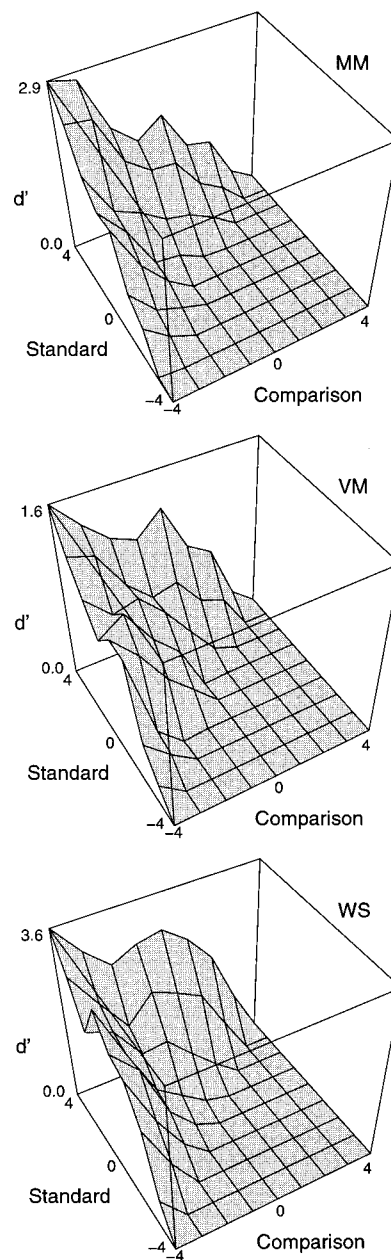


Fig. 5. Detectability d' of the difference between the standard and the comparison displacements (arcmin) for observers MM, VM, and WS. The display has motion noise. Note the different d' scale on each observer's plot.

surface is somewhat planar and tilted upward, as Eq. (4) would predict. The 95% confidence interval for the fitted standard deviation of the noise for MM's data is 2.88 ± 0.52 arc min; for VM it is 4.76 ± 0.33 arc min; and for WS it is 2.02 ± 0.25 arc min. The standard deviation of the motion noise in the display was 0.3 arcmin. Since the confidence intervals for the noise standard deviation do not include 0.3, all observers are clearly nonideal, their visual systems having additive noise with a standard deviation of approximately 4.5, 2.6 and 1.7 arcmin, respectively. In the noiseless experiment we found the internal noise standard deviation to be ~ 0.7 arcmin. So the standard deviation of the internal noise grows as the standard deviation of the external noise increases. The same effect has been found in the luminance domain.¹³ There are many possible explanations. One simple idea is that the observer tries to cope with the noisy stimulus by amplifying it, and the gain of this internal amplifier increases as the standard deviation of the display noise increases. The results of our study and the luminance domain study clash with those of Watamaniuk,¹⁴ who used a form of motion stimulus where each dot performed a two-dimensional random walk. He found that the internal-noise standard deviation did not depend on the standard deviation of the external noise. Perhaps the difference in Watamaniuk's result and our own is related to the form of noise used. In Watamaniuk's experiments, on each frame every dot received a different value of noise. In our experiments, on each frame every dot received the same value of noise. Our display was a rigid (though jittering) translation; Watamaniuk's was non-rigid.

The nonideal observer model's tilted plane fits the response surface quite well: The residuals (Fig. 6) are about half as big as they were for the noiseless displays. By adding motion noise to the displays, we have changed the residual plots dramatically. In the noiseless displays both observers' residual plots showed abrupt L-shaped ridges corresponding to better-than-predicted performance for motion detection. But now, with noisy displays (Fig. 6), these ridges are absent or have a different form. The residuals for MM are small and show no pattern, indicating that the nonideal observer model fits well. We explained the ridge in MM's noiseless data as being due to the action of a time-averaging or flicker mechanism. Since the ridge is now absent, the mechanism has been rendered inactive by the addition of motion noise. This result is consistent with the time-averaging idea, since motion noise will make the time-averaged output for both a static and a moving display consist of streaks (Fig. 4), resulting in poor performance. Motion noise would also inactive a flicker-based mechanism, since both static and moving displays with motion noise contain flicker.

For VM and WS the residuals show a broad peak: Performance is higher than predicted from the nonideal observer model for motion when one of the displacements is close to zero. The residual surface's broad peak is unlike the abrupt ridge found with the noiseless displays. We attributed the noiseless displays' ridge of high motion detection sensitivity to a time-averaging or flicker or Weber's law device. Perhaps such mechanisms are also

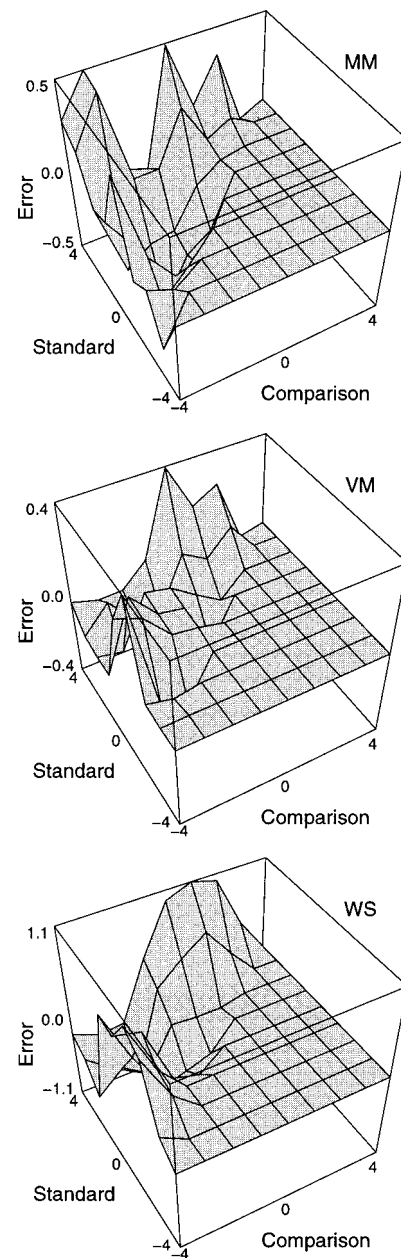


Fig. 6. Error (difference between observed and fitted d') as a function of the standard and the comparison displacements (arc-min) for observers MM, VM, and WS. The display has motion noise. Note the different error scale on each observer's plot.

partly behind the broad peak found with the noisy displays. However, we think that now a speed energy device has been engaged. A speed energy device squares and integrates the displacement or speed waveform delivered to it. Several previous results have pointed to such a speed energy device: the elliptical threshold loci found in a two-impulse temporal summation experiment,¹ the pedestal effect for speed discrimination,¹⁵ and the shape of directional tuning curves.¹⁶ (Note that speed energy is unrelated to Adelson and Bergen's¹⁰ motion energy.)

We now derive the predicted detectability surface from a speed energy mechanism. If the observer's visual system squares and sums the motion stimulus, the resulting

random variable is distributed as noncentral chi-squared. When signal s_0 is delivered, the mean is $\nu + a_0^2$ where ν is the number of samples and the variance is $2(\nu + 2a_0^2)$; when signal s_1 is delivered, the mean is $\nu + a_1^2$ and the variance is $2(\nu + 2a_1^2)$. For a large number of samples (as we used), the noncentral chi-squared distribution is well approximated by the normal. The measure d' is defined only for normal distributions with equal variances. However we could measure d'_e , which uses the average of the standard deviations, giving

$$d'_e = \frac{|a_1^2 - a_0^2|}{(2\nu + 2a_0^2 + 2a_1^2)^{1/2}}. \quad (9)$$

The output of this energy device is plotted in Fig. 7. Note the strong similarity between this plot and the residual plots of VM and WS in Fig. 6. It appears that in VM and WS an energy device is operating in parallel with a noisy but otherwise optimal detector (nonideal observer).

We have argued that motion noise abolishes the action of a supplementary time averaging or flicker mechanism. This occurs in all observers. We proposed that an energy device accounts for the residuals in observers VM and WS. Why is it not active in observer MM? There are two possible explanations. The first possibility is that further experimental trials would reduce the noise in MM's response surface and we would be able to observe an energy device's output in her residuals. The second possibility is that the deployment of any mechanism, including a speed energy mechanism, depends on the observer. We do not think that visual mechanisms are rigid, fixed, and universal to all observers. The observer develops the required mechanisms during the course of the experiment (perceptual learning) and chooses and combines mechanisms to produce the best performance. According to this point of view, MM either did not develop the speed energy mechanism or chose not to use it.

B. Efficiency of Motion Sensing

We measured the motion sensing efficiency of our observers on an absolute scale. The efficiency F , is defined^{17,18}

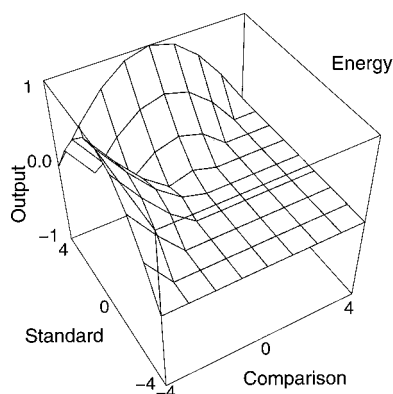


Fig. 7. Output of an energy detection mechanism as a function of the standard (a_0) and comparison (a_1) displacements. This model seems to explain the residual plots for VM and WS in Fig. 6.

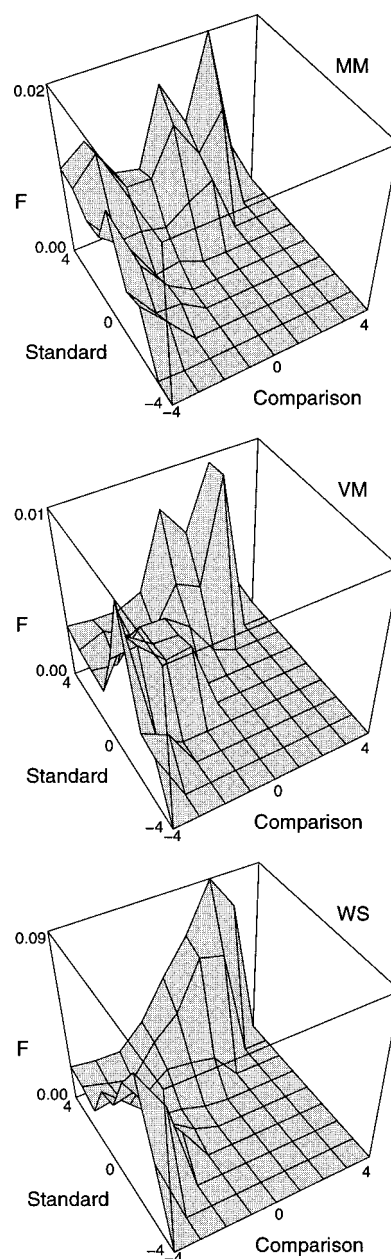


Fig. 8. Efficiency (F , the squared ratio of observed to ideal d') as a function of the standard and comparison displacements (arc-min) for observers MM, VM, and WS. The display has motion noise. Note the different efficiency scale on each observer's plot.

as

$$F = \left(\frac{d'_{\text{observed}}}{d'_{\text{ideal}}} \right)^2 \quad (10)$$

where d'_{ideal} is given by Eq. (4). The ideal observer adds no noise to the received stimulus, so if the stimulus is noiseless, then σ in Eq. (4) is zero. Thus in the noiseless case d'_{ideal} is infinite and the efficiency cannot be computed. By adding noise to the stimulus motion we are able to compute the efficiency surfaces for both observers (Fig. 8). For WS the maximum efficiency is near 9%, for MM it is about 2%, and for VM it is about 1%. We attribute the low efficiencies to internal noise added by the

observer to the stimulus (nonideal observer model). Another source of inefficiency is likely the extraction of the speed or displacement from the spatiotemporal luminance waveform (this extraction occurs perfectly in the ideal observer). Our efficiencies are similar to those of Watamaniuk,¹⁴ who compared data from real and ideal observers in an experiment where the random dots had a two-dimensional directional noise added onto their paths.

Now consider the shape of the efficiency surface. The ideal observer's efficiency is a flat plane at 100%, and a nonideal observer with additive internal noise would have a flat planar efficiency surface at some level below 100%. The efficiency surfaces of VM and WS have a distinctive twin-peak shape. This shape is similar to that seen in Fig. 7; we attribute it to the operation of a speed energy mechanism. MM's surface is irregular and tilted upward. This upward tilt implies that proportionately less noise is generated in MM's visual system for the larger displacements. This effect has been found in the luminance domain, where the observer's internal noise declines as retinal illuminance increases.^{19,20} We agree with Burgess²¹ that these seemingly low-level discrimination and detection tasks reveal high-level (cognitive) processing in the brain. If this is true, the sort of stimuli presented—luminance flashes or motion jumps—will not affect the operation of the information extraction and decision mechanisms that we are measuring, and we will find similar effects across stimulus domains. Why should such a noise-reduction-with-increasing-stimulus-magnitude effect be found in any domain? One possibility is that when the stimulus magnitude is increased, observer uncertainty about the signal's waveform parameters (time of the jump and its amplitude) is reduced. Observer uncertainty about a waveform that should ideally be known exactly makes the task one of detecting a signal with random parameters.

It is interesting to note that the direction discrimination task, studied widely in the D_{\max} literature,³ is the task humans are *least* efficient at.

5. CONCLUSIONS

We initially wondered whether human motion sensing was unitary, using one basic mechanism to discriminate moving displays, or whether instead it used a patchwork of mechanisms, each corresponding to one of the conventional motion tasks (motion detection, speed discrimination, and direction discrimination). Our data show that one basic mechanism, an ideal observer with added internal motion noise, accounts for most of human motion performance. This mechanism is unitary in that it cares only about the speed or displacement difference; the conventional motion task categories mean nothing to it. However, we also found evidence for other mechanisms that operate in parallel with the nonideal observer mechanism. The contribution of these other mechanisms is relatively small. When the display is noiseless, the secondary mechanism could be a Weber's law device or one that uses purely spatial (time-averaging) or temporal (flicker) information in the displays. When the display had added motion noise, we observed a secondary mechanism that computes the speed energy. This speed energy

mechanism is unitary and makes a small contribution to performance over the whole range of conventional motion tasks.

We derived an ideal observer model for the conventional motion tasks. Human performance differs from the ideal in two ways. First, the human visual system contains additive motion noise. This noise is likely due to variability in the outputs of the speed (or displacement) sensing neurons in the brain and to fixation variability. The standard deviation of the internal noise depends on the amount of external noise. Second, humans use ancillary mechanisms in addition to those used by an ideal observer.

ACKNOWLEDGMENTS

This work was supported by a grant from the Natural Sciences and Engineering Research Council of Canada.

Send all correspondence to William Simpson at the address on the title page or by e-mail: wsi@gcal.ac.uk.

REFERENCES

1. W. A. Simpson, "Temporal summation of visual motion," *Vision Res.* **34**, 2547–2559 (1994).
2. S. P. McKee, "A local mechanism for differential velocity detection," *Vision Res.* **21**, 491–500 (1981).
3. O. Braddick, "A short-range process in apparent motion," *Vision Res.* **14**, 519–527 (1974).
4. S. P. McKee and S. N. J. Watamaniuk, "The psychophysics of motion perception," in *Visual Detection of Motion*, A. T. Smith and R. J. Snowden, eds. (Academic, New York, 1994), pp. 85–114.
5. A. D. Whalen, *Detection of Signals in Noise* (Academic, New York, 1971).
6. W. M. Siebert, *Circuits, Signals, and Systems* (McGraw-Hill, New York, 1986).
7. G. Finley, "A high-speed plotter for vision research," *Vision Res.* **25**, 1993–1997 (1985).
8. R. M. Steinman, "Effect of target size, luminance, and color on monocular fixation," *J. Opt. Soc. Am.* **55**, 1158–1165 (1965).
9. R. P. Scobey and C. A. Johnson, "Displacement thresholds for unidirectional and oscillatory movement," *Vision Res.* **21**, 1297–1302 (1981).
10. E. H. Adelson and J. R. Bergen, "Spatiotemporal energy models for the perception of motion," *J. Opt. Soc. Am. A* **2**, 284–299 (1985).
11. W. Reichardt, "Autocorrelation, a principle for the evaluation of sensory information by the central nervous system," in *Sensory Communication*, W. A. Rosenblith, ed. (MIT Press, Cambridge, Mass., 1961), pp. 303–317.
12. D. Regan, "Form from motion parallax and form from luminance contrast: Vernier discrimination," *Spatial Vision* **1**, 305–318 (1986).
13. A. E. Burgess, "On observer internal noise," in *Application of Optical Instrumentation in Medicine XIV and Picture Archiving and Communication Systems (PACS IV) for Medical Applications*, R. H. Scheider and S. J. Dwyer III, eds., *Proc. SPIE* **626**, 208–213 (1986).
14. S. N. J. Watamaniuk, "Ideal observer for discrimination of the global direction of dynamic random-dot stimuli," *J. Opt. Soc. Am. A* **10**, 16–28 (1993).
15. W. A. Simpson, "Pedestal effect in visual motion discrimination," *J. Opt. Soc. Am. A* **12**, 2555–2563 (1995).
16. W. A. Simpson and A. Newman, "Motion detection and directional tuning," *Vision Res.* **38**, 1593–1604 (1998).
17. A. E. Burgess, R. F. Wagner, R. J. Jennings, and H. B.

- Barlow, "Efficiency of human visual signal discrimination," *Science* **214**, 93–94 (1981).
18. W. P. Tanner and T. G. Birdsall, "Definitions of d' and η as psychophysical measures," *J. Acoust. Soc. Am.* **30**, 922–928 (1958).
 19. N. S. Nagaraja, "Effect of luminance noise on contrast thresholds," *J. Opt. Soc. Am.* **54**, 950–955 (1964).
 20. D. G. Pelli, "The quantum efficiency of vision," in *Vision: Coding and Efficiency*, C. Blakemore, ed. (Cambridge U. Press, New York, 1990), pp. 3–24.
 21. A. E. Burgess, "High level visual decision efficiencies," in *Vision: Coding and Efficiency*, C. Blakemore, ed. (Cambridge U. Press, New York, 1990), pp. 431–440.